Trans Indian Inst Met (2020) 73(7):1925–1937
https://doi.org/10.1007/s12666-020-02007-6

ORIGINAL ARTICLE

A Kinetic Model for Chelating Extraction of Metals from Spent Hydrodesulphurization Catalyst by Complexing Agent

Orhon Alpaslan[1] · Ali Yaras[2] · Hasan Arslanoğlu[3]

Received: 15 November 2019 / Accepted: 15 May 2020 / Published online: 6 June 2020

Abstract In this present paper, chelating extraction of metals from spent hydrodesulphurization catalyst was carried out using ethylene diamine tetraacetic acid as complexing agent. Mo, Ni and Co metals were precipitated in ammonium molybdate, nickel dimethylglyoxime and cobalt hydroxide forms at pH:2, pH:6 and pH:10, respectively. The highest metal extraction yields (90.22% Mo, 96.71% Co, 95.31% Ni and 19.98% Al) were achieved under optimum process conditions. The activation energy values (E_a) of Co, Mo and Ni were calculated as 14.36 kJ/mol, 16.85 kJ/mol and 15.93 kJ/mol, respectively. It was determined that leaching kinetics fitted to the pseudo-first homogenous model and the chelating process was controlled by diffusion mechanism. In the light of the kinetic data, the kinetic equation including the process parameters was obtained as follows: $\ln(1-x) = 1.217 \times 10^{-4}[(C_A)^{1.068}(D)^{-0.929}(K/S)^{-0.850}\ (R)^{0.185}\exp(-6462.6/T)]t$. The results provided a new approach both for reducing the solid waste load of the petrochemical industry and for efficient recovery of metals from the spent hydrodesulphurization catalyst using EDTA.

Keywords Chelation · EDTA · Spent HDS catalyst · Complexing agent · Leaching · Metal recovery

1 Introduction

A large amount of solid catalysts are used in oil refineries to accelerate chemical reactions in catalytic processes [1]. Due to the accumulation of various impurities on the catalyst surface during refining, they lose their catalytic activity over time [2, 3]. The amount of spent catalyst in the world is estimated to be 170x10^3 tons per year [4]. It is known that they are very hazardous and harmful in terms of environment and human health [1, 5]. Therefore, valorization or storage of the spent catalysts is an important issue at the present time. The spent catalysts cannot be stored due to strict environmental requirements and large area requirements [2, 6]. It is not possible and economical to regenerate the catalysts that have lost their activity in the processes where thermal decomposition and phase separation occurs [7]. On the other hand, the spent catalysts can also be considered as secondary metal sources in terms of the metal contents. For this reason, it is preferable to reduce the environmental pollution, minimize the requirement for storage area and recovery of the metals to meet the metal needs of the market [8, 9].

The solid catalyst that loses catalytic activity during the sulfur removal process from crude oil is called hydrodesulphurization (HDS) spent catalyst and it is a hazardous product of petroleum industries in large quantities [4]. A great number of studies on hydrometallurgical, pyrometallurgical and bioleaching approaches to recover metals from the spent catalysts were reported in the literature [10–13]. Pyrometallurgy is a technique carried out at high temperatures using the suitable reagents for recovery

Electronic supplementary material The online version of this article (https://doi.org/10.1007/s12666-020-02007-6) contains supplementary material, which is available to authorized users.

✉ Ali Yaras
aliyaras@bartin.edu.tr; ayaras01@gmail.com

[1] Institute of Science and Technology, Bartin University, Bartin 74100, Turkey

[2] Department of Metallurgy and Materials Engineering, Bartin University, Bartin 74100, Turkey

[3] Department of Chemical and Process Engineering, Ahi Evran University, Kırsehir 40100, Turkey

Table 1 Chemical composition of the spent HDS catalyst

Element	% (wt.)
Al	37.94
Mo	9.35
Co	2.18
Ni	1.72
Ca	0.34
C	13.7
S	0.73
P	0.28
Others	0.051
Loss ignition (%)	33.709

of nonferrous metals from the spent catalyst [14–17]. However, it is also known that it releases certain toxic compounds and gases that cause serious pollution in case of smelting of the spent catalyst. Although metal recovery is realized in a short time, it is less preferred for recycling process due to high energy need and secondary pollution during the treatment. Although bioleaching is a hopeful technology for the recovery of metals from various solid wastes in recent years [18], it is not preferred because it requires a longer leaching time to achieve high extraction efficiency. The other considerations in biotechnological applications are possibility of losing the activity of microorganisms at high temperature and contamination of the environment [19]. The hydrometallurgy is the most favored process, namely chemical leaching, due to easy process control, short reaction time and high extraction efficiency for recovery of metals from various industrial wastes, soil and spent catalyst [20–29]. In the chemical leaching, the spent catalysts are treated with a series of chemical solutions such as sulfuric acid, oxalic acid and hydrochloric acid [25, 30–33]. In addition, the chemical leaching studies of the spent catalyst using hydrogen peroxide as oxidant with acids to further increase metal extraction efficiency and leaching time are reported in the literature [26, 34]. Although the hydrometallurgical method can be applied in terms of technical feasibility, the use of hazardous leaching agents is a major obstacle for further purification treatments [35]. This problem can be overcome by using safer and non-toxic organic lixiviants or metal chelating salts. The chelation is based on the formation of a highly soluble metal–ligand complex in the leaching medium [36]. The metal ions in the present complexes no longer react with other ions in the medium.

Chelation extraction of metals from the spent catalyst is an ecological approach in terms of waste management because it occurs at relatively low temperatures and the chelating agent used in the leaching process is biodegradable. In addition, because of non-corrosive medium and non-formation of any hazardous by-products over the process, the chelating technology is more preferable than other existing processes for metal extraction. It is known that organic chelating agents like nitrilotriacetic acid (NTA), ethylene diamine tetraacetic acid (EDTA) and diethylene triamine pentaacetic acid (DTPA) have high affinity and metal binding capacity for metals [36]. Of these compounds, EDTA is a well-known chelating agent that contains four carboxylates and two amino groups, which can form coordination complexes with metals, and is widely used in the metal extraction processes [37–43]. On the other hand, it is known that EDTA has high metal extraction efficiency and EDTA-metal complexes are thermodynamically stable [44, 45]. EDTA is an alternative complex agent for leaching because of obvious chelating affinities to different metal ions. For instance, nickel metal has been recovered from the spent catalyst in 96% yield in the form of nickel sulfate under the following experimental conditions: EDTA concentration 0.8 M, reaction temperature 100 °C, reaction time 10 h and pH:10 [46]. Vuyyuru et al. reported that 95% Ni metal was recovered from the spent catalyst at 150 °C and 4 h using EDTA in an autoclave system [47]. In another study, Co and Mo metals from spent HDS catalyst were recovered by 80.4% and 84.9% in the presence of EDTA, respectively [19]. As it is seen, the number of studies using EDTA as chelating agent in the extraction of metals from the spent catalysts is limited. Therefore, it is an important need to explore the chelating ability of EDTA in the extraction process of metals from the spent catalyst. The innovative aspect of this study is to recover Mo, Ni and Co metals from the spent HDS catalyst in high purity from ammonium molybdate, nickel dimethylglyoxime and cobalt hydroxide forms using EDTA in a two-step process: chelating reaction and chemical precipitation.

The present paper investigates the chelation extraction behavior of selected metals from the spent HDS catalyst in the presence of EDTA as a safe complexing agent. Also, the highest extraction rates were determined according to the solubility of metal oxides at different pH ranges. Optimum experimental conditions were determined and the process kinetics were examined in detail.

2 Material and Method

2.1 Material Characterization

HDS spent catalyst (Mo–Co–Ni/Al_2O_3) was provided by a petroleum plant in Romania. The analytical purity EDTA ($C_{10}H_{14}N_2Na_2O_8{\cdot}2H_2O$, ethylene diamine tetra acetic acid) used as complexing agent was purchased from Merck. The spent catalyst was crushed by a jaw crusher and grinded

Table 2 Values of surface area and pore volume of the spent HDS samples

Sample	Surface area (m^2/g)	Pore volume (ml/g)
Unroasted catalyst	131.9	0.876
Roasted catalyst	198.3	0.614
Leached catalyst	264.7	0.345

using ball mill. The powder sample was separated into different particle sizes (20, 30, 75, 150, 300 and 600 μm) by sieving. The spent HDS catalyst was released in the desulfurization process in oil refineries and sulfur accumulated on the catalyst surface. The roasting process was carried out to easily oxidize the sulfur in the spent HDS catalyst under atmospheric conditions using the oven with 10 °C/min heating rate at 600 °C and 180 min. [48]. The roasted samples were stored in plastic containers for chelation experiments.

The chemical composition of the spent HDS catalyst is given in Table 1. The surface morphology and elemental contents of the samples at before/after the roasting process and the solid residue after the leaching were determined by SEM–EDS (Tescan-MAIA3 XMU). Based on the results in Fig. 1, the samples have different particle sizes and no homogeneous distribution. On the other hand, the amount of sulfur and carbon in the catalyst structure before roasting is higher than the amount of sulfur and carbon in the catalyst after roasting. This is because the sulfur and carbon elements are removed from the structure in the form of sulfur dioxide (SO_2) and carbon dioxide (CO_2) gases under high temperature.

2.2 Leaching Experiments

The chelation experiments were carried out in 250-ml Erlenmeyer using incubator (ZCHENG 200D) with controlled temperature and stirring speed. In order to optimize the process conditions, the effects of particle size, liquid/solid ratio, EDTA concentration, leaching temperature, leaching time and stirring speed on the dissolution of selected metals from spent HDS catalyst were investigated, respectively. For the optimization of any process parameter, experiments were performed with single factor by keeping all other parameters constant. EDTA solutions were added to the flasks and then the solution pHs were measured. After the solution temperature reached the desired temperature, the samples were added to the solution and stirred. Following a certain reaction time, the leachate samples were filtered and the metal concentration passed to the solution was analyzed using a atomic absorption spectrophotometry (Perkin Elmer AAnalyst-400) and ICP-MS (Agilent 7500ce). All experimental results are given as mean values with standard deviations. The flowchart of the chelant-assisted metal extraction process is presented in Fig. 2.

The results in Table 2 indicate that the surface area of the samples increases and the pore volume decreases as a result of roasting and leaching processes.

The phases analysis of samples were carried out by XRD (Rigaku-Smartlab). As seen in Fig. 3, it is complex and shows the presence of metal oxide phases such as Al_2O_3, Ni_2O_3, MoO_2 and CoO.

2.3 Chemical Precipitation

The recovery of metals selected from leachate liquor under optimum process conditions was carried out by progressive precipitation method. The chemical precipitation method is based on the precipitation of selected metal ions at desired pH value in consequence of addition of various chemicals to the leaching medium. Mo in the leached sample was precipitated at pH:6 using ammonia. Precipitation of Ni was carried out at pH 6–6.5 by adding NaOH. The pH of the leached solution was adjusted to pH:9–9.5 with NaOH and Co was precipitated. During the precipitation treatments, the pH adjustments were carried out using 0.1 M H_2SO_4 and 0.1 M NaOH. The solid precipitates were filtered and the metal precipitation yield was analyzed by ICP-MS. The purities of the precipitates at different pH values for all metals (Mo, Co, Ni and Al) were determined on average at 95%.

2.4 Metal-Chelate Complex Formation Reactions

When chelating agent (L^{-4}) is added to the solid–liquid interface in a chelate-assisted metal extraction process, metal–chelate complexes (M_i–L^{-2}) are formed on the catalyst surface and then they pass from solid surface into solution according to Eq. (1). {[HDS]-O} refers to active sites on the catalyst surface, M_i^{+2} represents the metal that interacts with the ligand, M_{ii}^{+2} represents other metals in the solution. If metal oxides and hydroxides are present in the solution medium, they are partially soluble in the presence of chelate agent (Eqs. 3 and 4) [19, 49, 50].

Table 3 Reaction rate constants and regression coefficient values of kinetic model

Parameter	Pseudo-first order kinetic model					
	Co		Mo		Ni	
	k (min^{-1})	R^2	k (min^{-1})	R^2	k (min^{-1})	R^2
Particle size (μm)						
1200	0.0093	0.99	0.0114	0.9763	0.0098	0.998
600	0.0137	0.9985	0.0163	0.9966	0.0148	0.9985
300	0.0218	0.9988	0.0257	0.9973	0.0244	0.9984
150	0.0352	0.9994	0.0401	0.9974	0.0383	0.9992
75	0.0491	0.9973	0.0589	0.997	0.0561	0.982
30	0.0707	0.9927	0.0797	0.9897	0.0747	0.996
L/S ratio (ml/g)						
5	0.0037	0.991	0.0022	0.989	0.0089	0.995
7.5	0.0080	0.993	0.0061	0.996	0.0214	0.991
10	0.0123	0.999	0.0089	0.994	0.0321	0.999
12.5	0.0135	0.998	0.0105	0.997	0.0374	0.995
15	0.0196	0.997	0.0150	0.994	0.0517	0.993
17.5	0.0215	0.992	0.0166	0.987	0.0552	0.983
20	0.0246	0.996	0.0172	0.986	0.0570	0.982
EDTA concentration (M)						
0.025	0.0068	0.9916	0.0066	0.9905	0.0062	0.9906
0.05	0.0135	0.9913	0.0128	0.9942	0.0133	0.9924
0.1	0.026	0.9945	0.0215	0.9984	0.0227	0.9975
0.15	0.037	0.9943	0.030	0.9993	0.0348	0.9958
0.2	0.0477	0.9979	0.0341	0.0998	0.0383	0.9997
0.25	0.0556	0.9985	0.0385	0.994	0.0485	0.9984
Temperature (^oC)						
10	0.0695	0.9956	0.0544	0.9975	0.0555	0.9945
20	0.0939	0.9948	0.0870	0.9898	0.1037	0.9901
30	0.1491	0.9979	0.1349	0.9956	0.1584	0.9934
40	0.2388	0.9909	0.2045	0.9989	0.2565	0.9971
50	0.2839	0.996	0.2849	0.9994	0.3208	0.9974
60	0.4159	0.9981	0.4372	0.9983	0.5041	0.9997
Stirring speed (rpm)						
50	0.0088	0.99	0.0068	0.9942	0.0049	0.9901
100	0.0121	0.985	0.0120	0.9894	0.0080	0.9899
200	0.0193	0.989	0.0155	0.9923	0.0124	0.9909
300	0.0259	0.987	0.0214	0.9908	0.0189	0.9898
400	0.0303	0.992	0.0256	0.9939	0.0227	0.9895
500	0.0331	0.994	0.0280	0.9954	0.0242	0.9952
600	0.0402	0.998	0.0300	0.9971	0.0262	0.9993

$$\{[\mathrm{HDS}]\text{ - O}\} - \mathrm{M}_i^{+2} + \mathrm{L}^{-4} + \mathrm{H_2O} \leftrightarrow \mathrm{HDS} - \mathrm{OH} + \mathrm{M}_i - \mathrm{L}^{-2} + \mathrm{OH}^- \quad (1)$$

$$\mathrm{M}_i(\mathrm{OH})_2 + \mathrm{L}^{-4} \leftrightarrow \mathrm{M}_i - \mathrm{L}^{-2} + 2\mathrm{OH}^- \quad (2)$$

$$\mathrm{M}_i\mathrm{O} + \mathrm{L}^{-4} + \mathrm{H_2O} \leftrightarrow \mathrm{M}_i - \mathrm{L}^{-2} + 2\mathrm{OH}^- \quad (3)$$

In the presence of metal–chelate complexes on the catalyst surface, they can be replaced with other adsorbed metals (Eqs. 5 and 6) or re-adsorbed by surface complexation (Eq. 4). However, these phenomena may

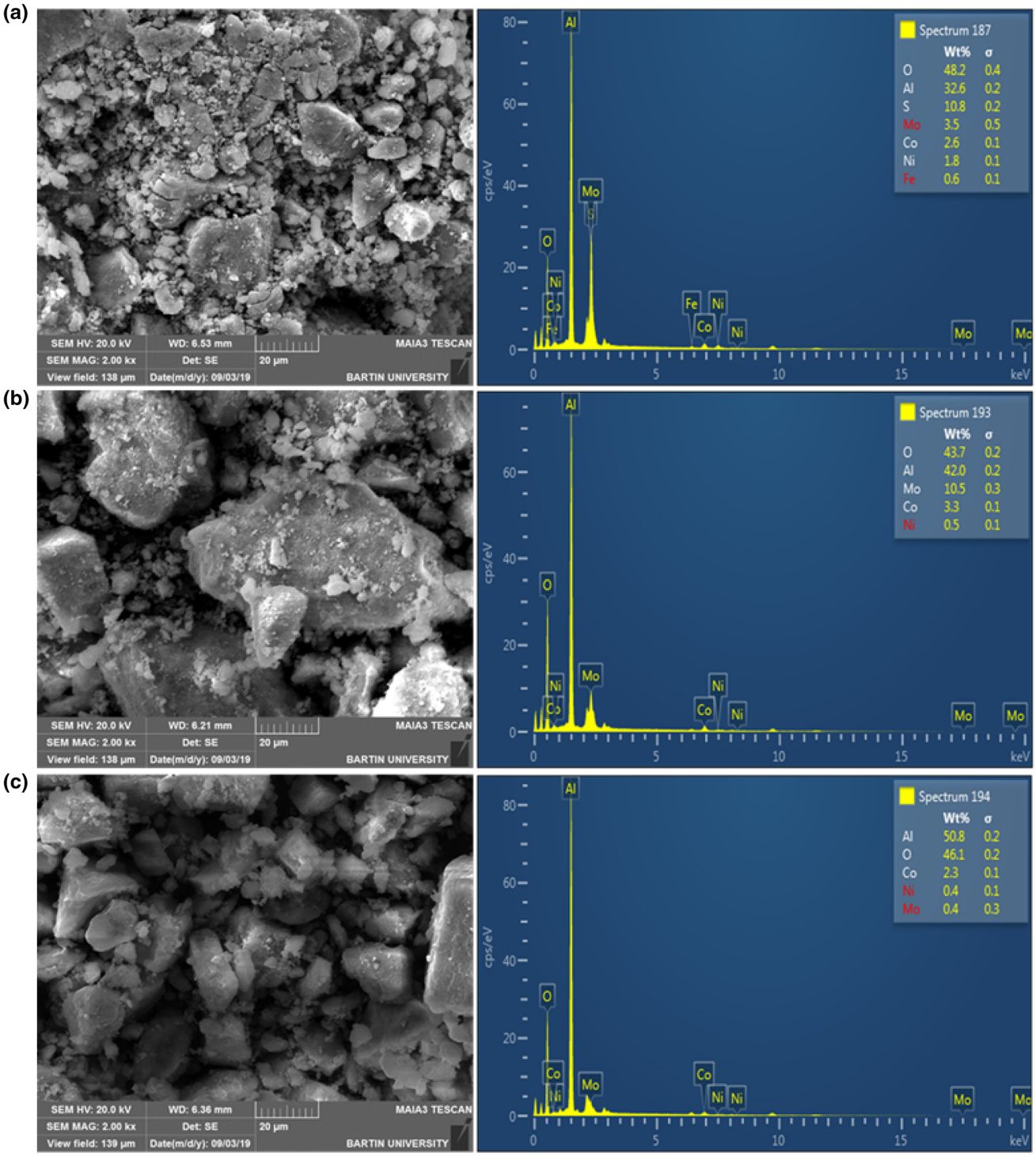

Fig. 1 SEM-EDS results of **a** raw spent catalyst, **b** roasted spent catalyst and **c** leaching residue of spent catalyst

occur depending upon the stability of the metal–chelate complexes, bonding strength of M_i^{+2} and accessibility of M_{ii}^{+2} [49, 51, 52].

$$[\mathrm{HDS}] - \mathrm{OH} + \mathrm{M}_i - \mathrm{L}^{-2} \leftrightarrow [\mathrm{HDS}] - \mathrm{L} - \mathrm{M}_i + \mathrm{OH}^- \quad (4)$$

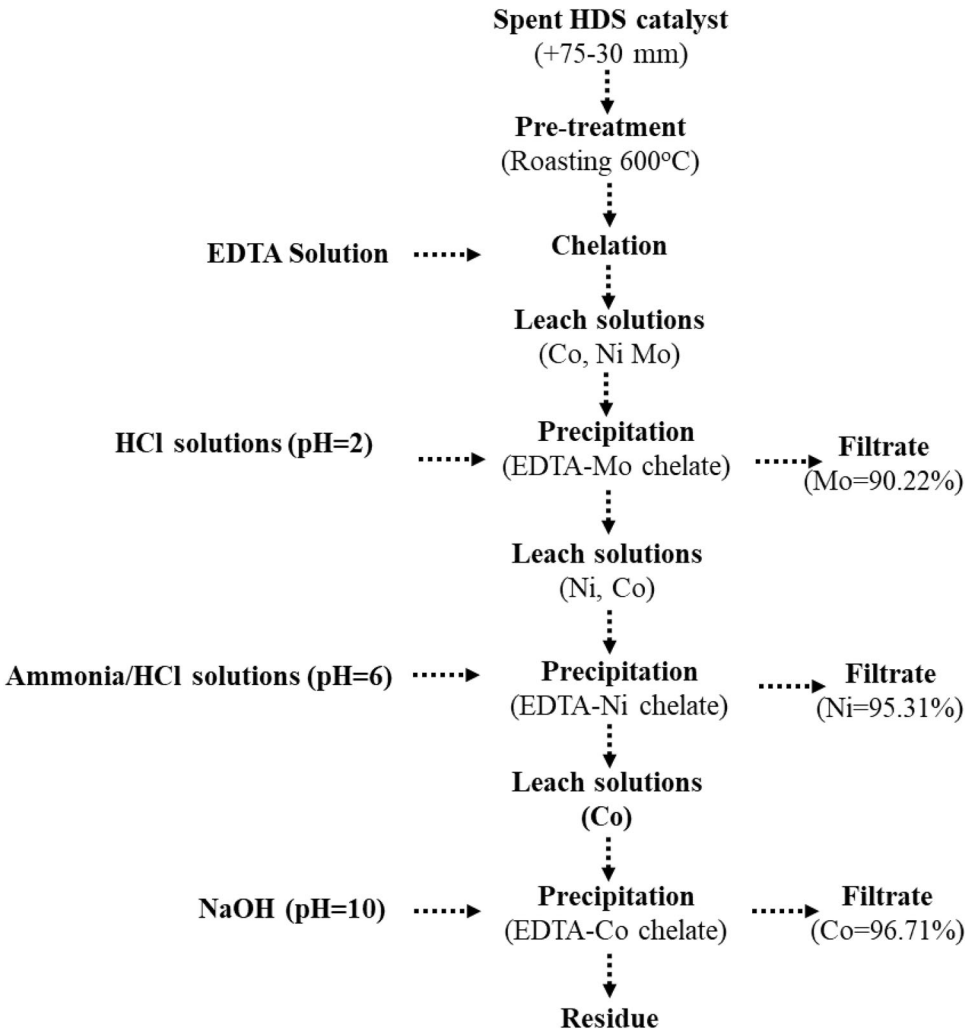

Fig. 2 The flowchart of the chelation extraction process of metals

$$[\mathrm{HDS}]-\mathrm{L}-\mathrm{M}_i+[\mathrm{HDS}]-\mathrm{O}-\mathrm{M}_{ii}^{+} \leftrightarrow [\mathrm{HDS}]-\mathrm{L}-\mathrm{M}_{ii}+[\mathrm{HDS}]-\mathrm{OH}+\mathrm{M}_i^{+} \quad (5)$$

$$[\mathrm{HDS}]-\mathrm{L}-\mathrm{M}_{ii}+\mathrm{OH}^{-} \leftrightarrow [\mathrm{HDS}]-\mathrm{OH}+\mathrm{M}_{ii}-\mathrm{L}^{-2} \quad (6)$$

The chelating reaction between EDTA and metals occurs as denoted in Fig. 4.

3 Results and Discussions

3.1 Effect of Particle Size

The leaching experiments carried out between the particle size range of $-1200+600$ µm and $-30+20$ µm to examine the effect of internal mass transfer resistance. The results are shown in Fig. 5. It presents that the leaching efficiency is increased as the particle size decreases. In consequence of the reduction in particle size from 150 µm to 30 µm, the extraction efficiencies of Mo, Al, Co and Ni metals increase from 12.63%, 2.63%, 16.35% and 15.89% to 76.71%, 16.70%, 77.86% and 78.55%, respectively. An important influence of particle size on dissolution efficiency reveals that internal diffusion is dominant on the leaching process [53]. On the other hand, there is no significant increase in the dissolution rates of metals in case of particle size smaller than 150 µm. This means that the internal mass transfer resistance is negligible of any particle size below 150 µm. Further experiments were performed in the range of 150 µm in terms of optimum particle size.

3.2 Effect of Liquid/Solid Ratio

Figure 6 demonstrates the effects of L/S ratio on the chelating extraction efficiencies of metals from spent HDS catalyst. At L/S: 5 ml/g, leaching efficiencies of metals (23.27% Mo, 4.92% Al, 29.10% Co and 25.28% Ni) are very low because of the low rate of chelating reaction. When the leaching efficiencies of metals are increased gradually up to L/S: 15 ml/g, the extraction yields of Mo,

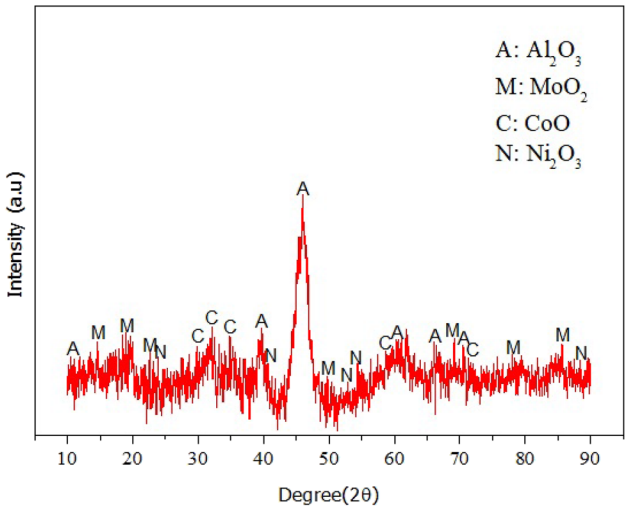

Fig. 3 XRD patterns of the roasted spent HDS catalyst

Al, Co and Ni reach up to 80.99%, 18.24%, 85.43% and 82.43%, respectively. It can be attributed to the number of cationic ions available in the leaching system. This means that the number of protons in the leaching medium is sufficient to react with the metals in the spent HDS catalyst at high L/S ratios [54]. The viscosity of the solid–liquid mixture is reduced at higher L/S ratios. Thus, a homogeneous mixture is obtained, the diffusion layer thickness around the particle is reduced and there is an increase in leaching efficiency [55]. However, in our study, there is no marginal increase in the chelating extraction values of metals with the increase of L/S ratio to 20 (83.33% Mo, 18.3% Al, 88.83% Co and 85.53% Ni). Similar observations have been reported by Chauhan et al. in the literature [19]. In another example, it has been reported that the leaching efficiency of Ni metal from the spent catalyst increases from 23 to 90% by increasing the L/S ratio from 5 to 50 [46]. Also, when the desired value of L/S ratio is reached in terms of the maximum metal extraction efficiency, an excess of the chelating agent in the leaching medium may decrease the yield [56]. On the other hand, the use of plenty of chelating agent to achieve high L/S ratios is not economically feasible. Therefore, subsequent experiments were carried out at L/S: 5 ml/g to achieve maximum metal extraction efficiency.

3.3 Effect of EDTA Concentration

The concentration of chelating agent plays a crucial role in leaching process. Figure 7 shows the influence of EDTA concentration on chelating extraction of metals from spent HDS catalyst.

With increasing EDTA concentration from 0.025 M to 0.15 M, it is clear that the leaching yields of Mo, Al, Co and Ni metals increases from 10%, 20%, 30% and 40% to 83.26%, 18.63%, 89.13% and 87.60%, respectively. At higher of EDTA concentrations, there is no significant change in the amount of metal passing to the leaching solution compared to EDTA concentration of 0.15 M. Therefore, the optimum EDTA concentration has been selected to be 0.15 M and further chelating extraction experiments are performed at 0.15 M EDTA concentration. Verma and Hait [57] reported that a similar trend was observed in metal extraction efficiencies from e-waste with increasing DTPA concentration from 0.3 to 0.5 M, and leaching efficiency dramatically dropped with further of DTPA concentration (0.7 M).

3.4 Effect of Leaching Temperature and Time

A series of experiments were performed at different leaching temperatures to study the effect of temperature which is an extremely important parameter for leaching efficiency and kinetics.

The extraction efficiencies of metals gradually increases as the reaction temperature from 10 to 40 °C as shown in Fig. 8. With the reaction temperature rising from 10 to 40 °C, the extracted metal ratios of Mo, Al, Co and Ni are achieved from 25.41%, 5.51%, 33.10% and 28.55% to 81.22%, 19.68%, 86.35% and 85.0%, respectively. This trend in chelation extraction efficiencies of metals due to the increase in reaction temperature can be explained by Arrhenius equation. The raise in the reaction temperature, which is directly related to leaching kinetic, improves the number and chance of molecular collision in the leaching medium and consequently enhances the metal extraction yield. The similar results of the numerous leaching applications using solid wastes containing various metals have been reported by researchers [19, 57–59]. The leaching temperature for next experiments has been considered to be 40 °C. As seen in Fig. 9, the dissolution percentages of Mo, Al, Co and Ni metals increase rapidly to 60 min. and reach 87.57%, 20.46%, 95.96% and 94.13%, respectively. At longer leaching times and higher temperatures, no significant increase in metal extraction rates is observed.

3.5 Effect of Stirring Speed

The stirring speed is an important parameter affecting the mass transfer rate between the solid–liquid phases in the leaching reactions. The effect of stirring speed on chelation extraction rates of metals is given in Fig. 10. A substantial increase is observed up to 300 rpm, the extraction of Mo, Al, Co and Ni metals at that stirring speed is determined as 90.22%, 19.98%, 96.71% and 95.31%, respectively. However, beyond stirring speed of 300 rpm, since the diffusion layer thickness around the solid particle does not

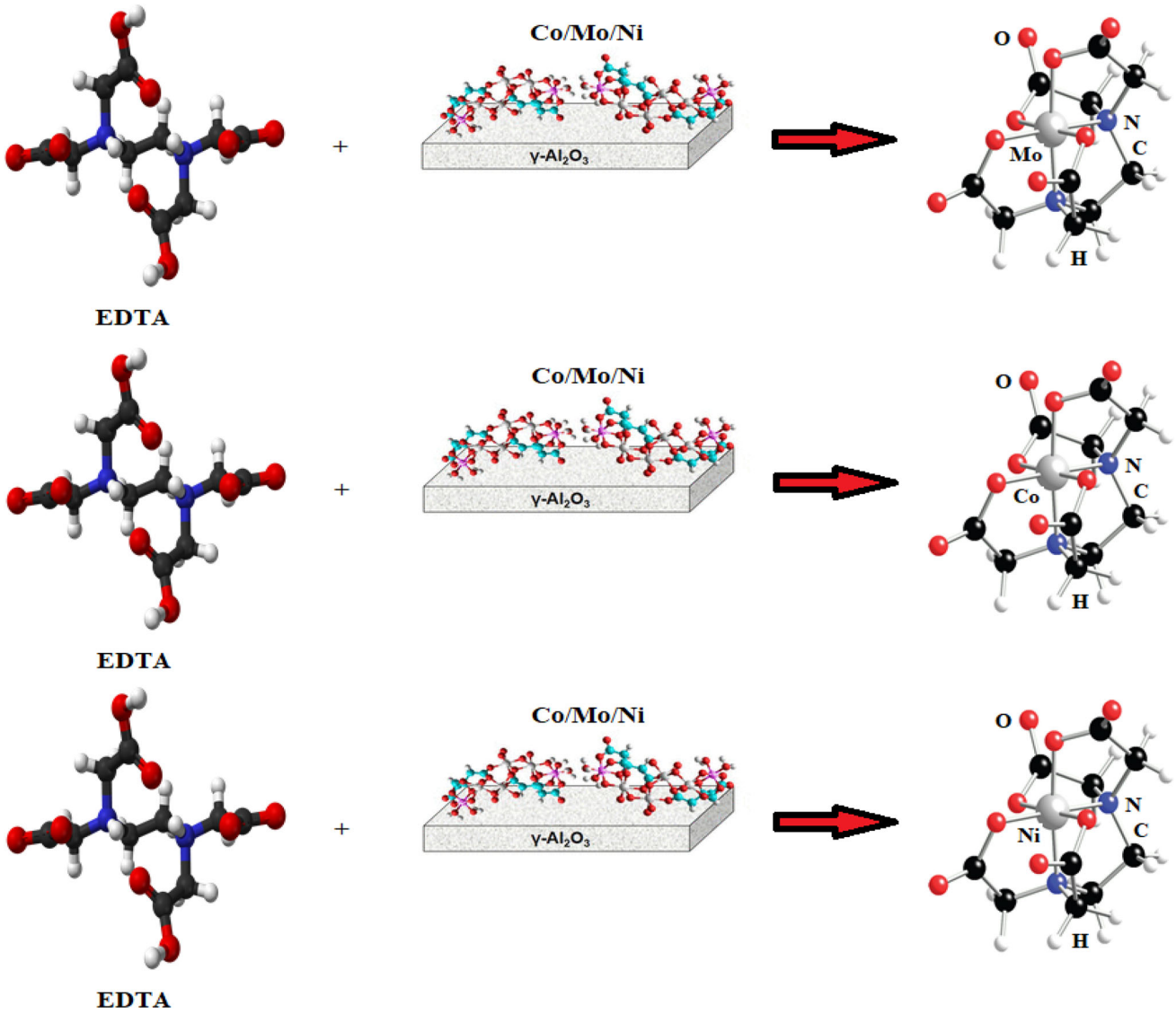

Fig. 4 Chelating reaction of EDTA with metal ions

significantly affect the reaction rate, only an increase of 3% is observed in the metal extraction efficiencies. It may be attributed to the more efficient mass transfer up to stirring speed of 300 rpm. As a result of increasing stirring speed, the interaction between the solid phase and the liquid phase generally improves and extraction efficiency increases. The experimental data are in good agreement with the results of other researchers in the literature [58, 59]. Because of no significant increase in metal extraction efficiencies at stirring speeds higher than 300 rpm, the optimum stirring speed for following chelation extraction experiments is determined to be 300 rpm.

It is clearly seen that the dissolution rate of Al (19.98%) is considerably lower than other metals under the optimum leaching conditions. As is known, aluminum production from high alumina-containing bauxite ore is only achieved in the concentrated alkaline medium and under high temperature and pressure conditions [60]. The amount of

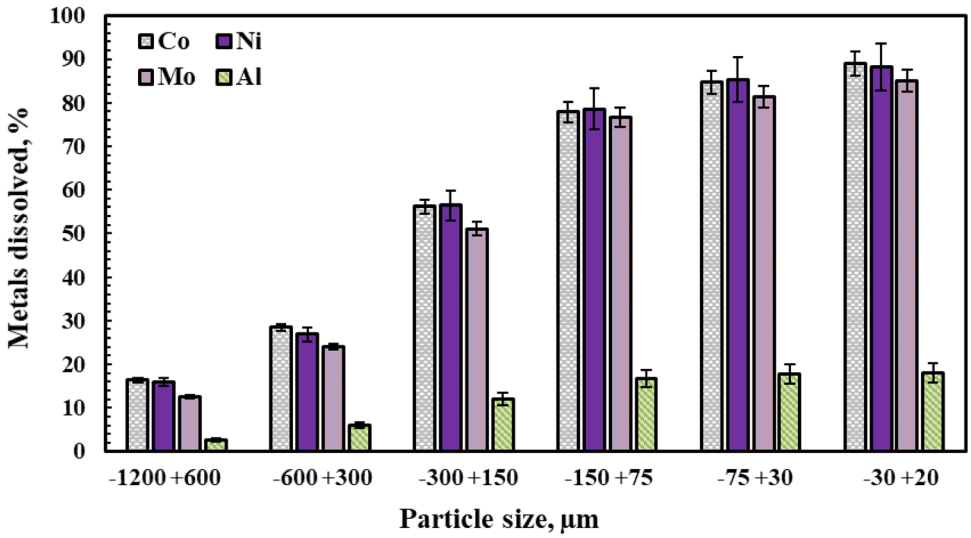

Fig. 5 Effect of particle size on metal dissolution rates [L/S ratio: 12.5 ml/g; EDTA concentration: 0.2 M; leaching temperature: 20 °C; leaching time: 60 min; stirring speed, 200 r/min]

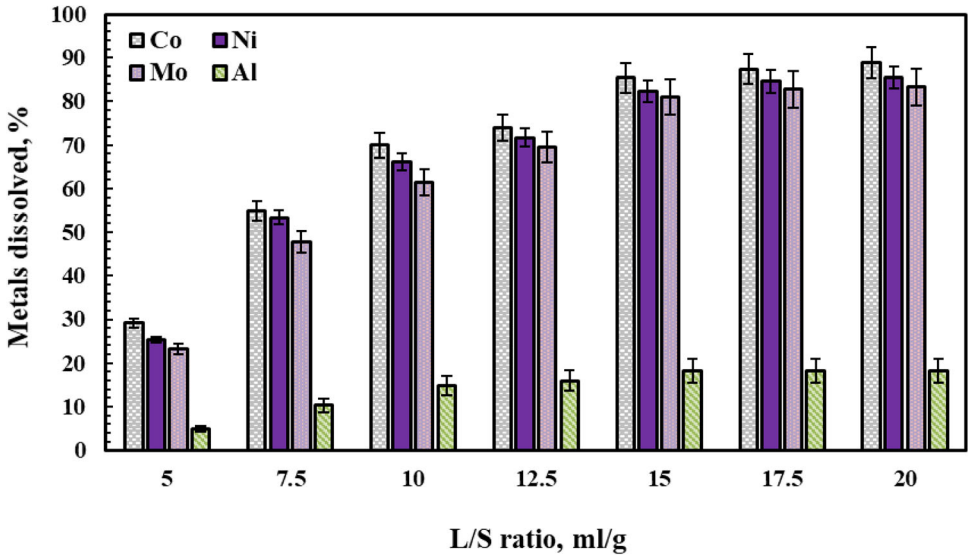

Fig. 6 Effect of liquid/solid ratio on metal dissolution rates [Particle size: + 75 − 30 µm; EDTA concentration: 0.2 M; leaching temperature: 20 °C; leaching time: 60 min; stirring speed, 200 r/min]

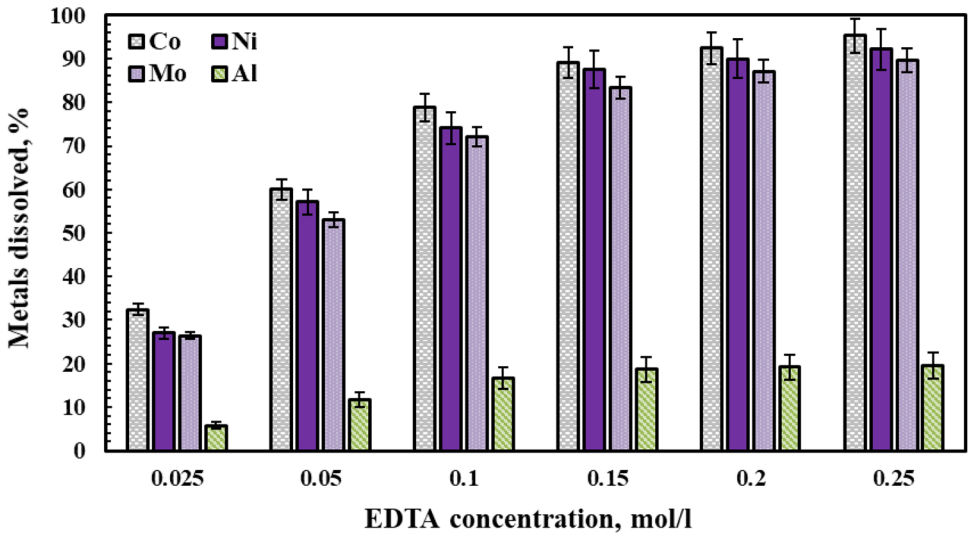

Fig. 7 Effect of EDTA concentration on metal dissolution rates [Particle size: + 75 − 30 µm; L/S ratio: 15 ml/g; leaching temperature: 20 °C; leaching time: 60 min; stirring speed, 200 r/min]

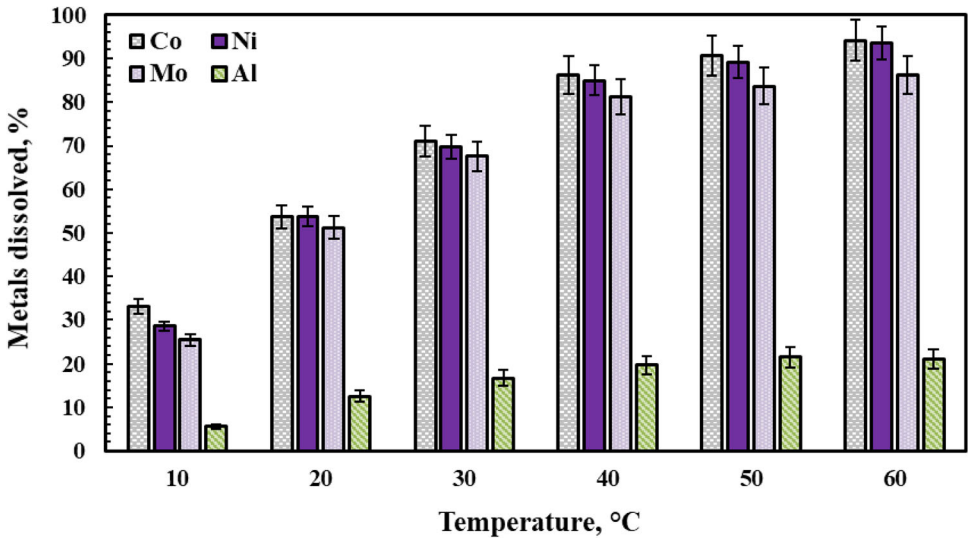

Fig. 8 Effect of leaching temperature on metal dissolution rates [Particle size: + 75 − 30 μm; L/S ratio: 15 ml/g; EDTA concentration: 0.2 M; leaching time: 60 min; stirring speed, 200 r/min]

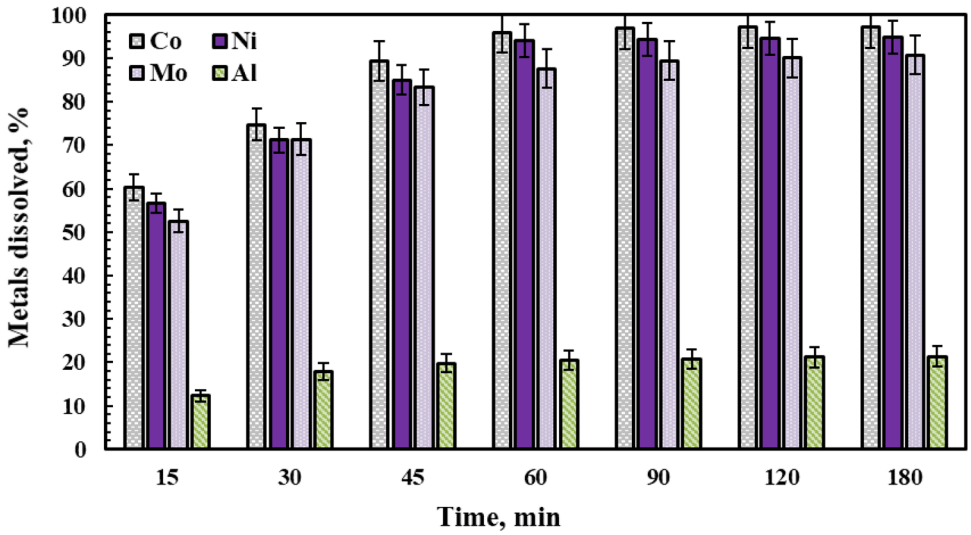

Fig. 9 Effect of leaching time on metal dissolution rates [Particle size: + 75 − 30 μm; L/S ratio: 15 ml/g; EDTA concentration: 0.2 M; leaching temperature: 60 °C; stirring speed, 200 r/min]

aluminum dissolved is limited since the leaching process has been carried out at atmospheric pressure, low EDTA concentration and lower temperatures in this study.

3.6 Kinetic Analysis

The reaction between the spent HDS catalyst and EDTA solution is a heterogeneous reaction in the solid–liquid phases. The kinetic analysis of such reactions is generally carried out using non-catalytic solid–fluid heterogeneous reaction models. The shrinking core model is often preferred to determine the rate-limiting stage in kinetic analysis of leaching/dissolution reactions [61, 62]. During the leaching reactions, a change in particle size may be observed, that is, it may remain constant or decrease. The reaction rate can be controlled by one or more steps in the heterogenous reaction models: the fluid film, diffusion, chemical reaction or diffusion from the product layer. Reaction rate equations of these models are already described in the literature [63, 64]. The homogeneous model assumes that the leaching reagent penetrates the solid particle and reacts with the particle. The reaction rates under these conditions can be represented by pseudo-first or pseudo-second homogeneous models [64]. The kinetic analysis of the experimental results with homogeneous and heterogeneous models reveals that the present process is in agreement with the homogeneous model. For this process, pseudo-homogeneous models have been applied and it is observed that the most suitable model to represent the dissolution kinetics of chelating extraction of metals from the spent HDS catalyst in the presence of EDTA solution is the first order pseudo-homogeneous kinetic in Eq. (7).

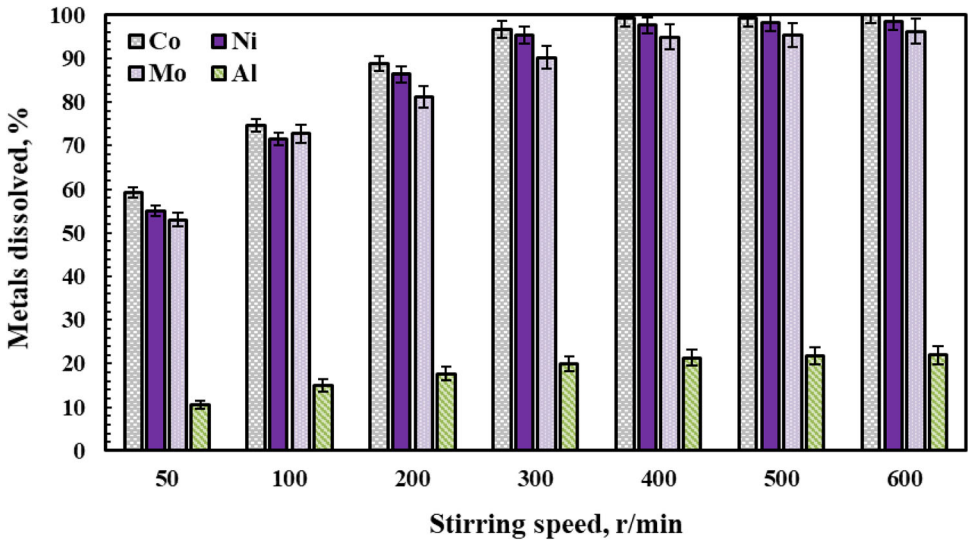

Fig. 10 Effect of stirring speed on metal dissolution rates [Particle size: + 75 − 30 μm; L/S ratio: 15 ml/g; EDTA concentration: 0.2 M; leaching temperature: 60 °C; leaching time: 60 min]

$$-\ln(1-x) = k.t \tag{7}$$

x is the conversion fraction, k is the reaction apparent rate constant and t is the reaction time (min). Based on Eq. (7), the graphs of EDTA concentration, particle size, L/S ratio, stirring speed and reaction temperature are plotted (see electronic supplementary Figure S1, Figure S2, Figure S3, Figure S4 and Figure S5). The straight lines passing through the origin are obtained from these graphs. Therefore, the kinetic equation of the process can be expressed as follows (Eq. 8);

$$\ln(1-x) = k\left[(C)^a(D)^b\left(\frac{L}{S}\right)^c(R)^d\exp^{\left(-\frac{E_a}{RT}\right)}\right]t \tag{8}$$

C, D, R, L/S and *T* denote EDTA concentration, particle size, stirring speed, L/S ratio and reaction time, respectively. *a, b, c* and *d* are calculated from apparent rate constants of related parameters. The constants of *a, b, c* and *d* are found to be 0.9189, − 0.5678, 1.3334, 0.6126; 0.7673, − 0.5489, 1.4435, 0.5917 and 0.8749, − 0.5719, 1.3243, 0.6988 for Co, Mo and Ni, respectively. With the reaction rate constants obtained from the results in Fig. 11, according to the Arrhenius equation, the activation energies of the chelating reactions of Co, Mo and Ni metals are calculated as 14.36 kJ/mol, 16.85 kJ/mol and 15.93 kJ/mol, respectively (Fig. 11). Consequently, using the results in Table 3, the kinetic expression (Eq. 9) containing the process parameters can be written as follows:

$$\ln(1-x) = 1.217\times10^{-4}[(C_A)^{1.068}(D)^{-0.929}\left(K/S\right)^{-0.850}(R)^{0.185}\exp(-6462.6/T)\Big]t \tag{9}$$

It is reported in the literature that the activation energy value will be higher than 40 kJ/mol to control a process by the chemical reaction, and it will be less than 40 kJ/mol to control the diffusion mechanism [57, 65]. Since the correlation coefficients (R^2) in the plotted graphs according to Arrhenius equation of each metals is at least 0.99 (Fig. 11), the activation energy values indicate that the chelating extraction process is diffusion controlled.

4 Conclusions

The optimum process conditions for the maximum chelating extraction of metals from the spent catalyst are determined as follows: particle size: + 75 − 30 μm; L/S ratio: 15 ml/g; EDTA concentration: 0.2 M; leaching temperature: 60 °C and leaching time: 60 min. The selective separation of each metal has been performed by a pH-controlled precipitation technique. Mo, Ni and Co have been precipitated at pH:2, pH:6 and pH:10, respectively. The maximum extraction of 90.22% Mo, 96.71% Co, 95.31% Ni and 19.98% Al is obtained in presence of EDTA at optimum leaching conditions. According to the results of the kinetic analysis, the chelating extraction process represents the first order pseudohomogeneous reaction model and the rate control step is the diffusion. The activation energies of Co, Mo and Ni metals have been calculated as 14.36 kJ/mol, 16.85 kJ/mol and 15.93 kJ/mol, respectively. In the light of the kinetic data, the kinetic equation including the process parameters is obtained as follows: $\ln(1-x) = 1.217\times10^{-4}[(C_A)^{1.068}(D)^{-0.929}(K/S)^{-0.850}(R)^{0.185}\exp(-6462.6/T)]t$. For the extraction of metals from the spent catalyst, a two-stage process can be applied as follows: chelating reaction and chemical precipitation. The most important aspect of chelating extraction processes is the recyclability of the chelating agent. In this sense, more than 90% of EDTA may be

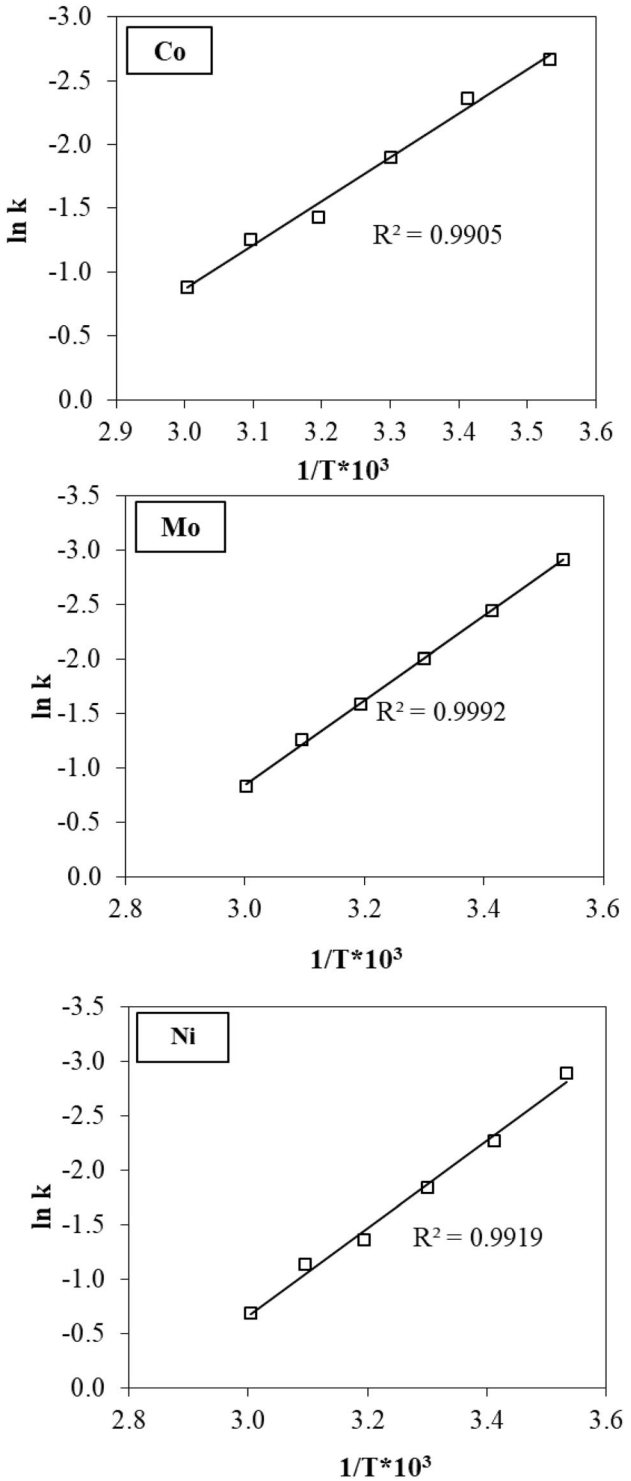

Fig. 11 lnk versus 1/*T* graph

recycled by the dechelation process for 8 h at room temperature. To increase the EDTA recovery, the metal solution is then precipitated by keeping under cold conditions for 2 days. Meanwhile, the natural solubility of EDTA may cause 2–3% EDTA loss in metal solution [19, 47].Therefore, further studies should focus on recycling of chelating agents, the synthesis and applicability of new chelating agents. Also, industrial inspection of the present process under optimum conditions may allow chelating technology to replace primitive techniques for metal recovery from secondary metal sources such as the spent catalyst.

Acknowledgements This paper was produced from Orhon ALPASLAN's master thesis.

References

1. A. Akcil, F. Vegliò, F. Ferella, M. D. Okudan, and A. Tuncuk, Waste Manag. **45**, 420 (2015).
2. M. Marafi and A. Stanislaus, Resour. Conserv. Recycl. **52**, 859 (2008).
3. M. Marafi and A. Stanislaus, Resour. Conserv. Recycl. **53**, 1 (2008).
4. P. Dufresne, Appl. Catal. A Gen. **322**, 67 (2007).
5. C. Liu, Y. Yu, and H. Zhao, Fuel Process. Technol. **86**, 449 (2005).
6. L. E. Macaskie, I. P. Mikheenko, P. Yong, K. Deplanche, A. J. Murray, M. Paterson-Beedle, V. S. Coker, C. I. Pearce, R. Cutting, and R. A. D. Pattrick, Hydrometallurgy **104**, 483 (2010).
7. A. Marafi, S. Fukase, M. Al-Marri, and A. Stanislaus, Energy & Fuels **17**, 661 (2003).
8. H. Srichandan, S. Singh, K. Blight, A. Pathak, D. J. Kim, S. Lee, and S. W. Lee, Int. J. Miner. Process. **134**, 66 (2015).
9. M. Motaghed, S. M. Mousavi, S. O. Rastegar, and S. A. Shojaosadati, Bioresour. Technol. **171**, 401 (2014).
10. J. Ramos-Cano, G. González-Zamarripa, F. R. Carrillo-Pedroza, M. de Jesús Soria-Aguilar, A. Hurtado-Macías, and A. Cano-Vielma, Int. J. Miner. Process. **148**, 41 (2016).
11. S. Huang, J. Liu, C. Zhang, B. Hu, X. Wang, M. Wang, and X. Wang, JOM **71**, 4681 (2019).
12. N. Nagar, H. Garg, and C. S. Gahan, Biocatal. Agric. Biotechnol. **20**, 101252 (2019).
13. S. Vyas and Y.-P. Ting, Chemosphere **160**, 7 (2016).
14. B. B. Kar, P. Datta, and V. N. Misra, Hydrometallurgy **72**, 87 (2004).
15. B. B. Kar, B. V. R. Murthy, and V. N. Misra, Int. J. Miner. Process. **76**, 143 (2005).
16. M. H. Shariat, N. Setoodeh, and R. A. Dehghan, Miner. Eng. **14**, 815 (2001).
17. D. D. Sun, J. H. Tay, H. K. Cheong, D. L. K. Leung, and G. Qian, J. Hazard. Mater. **87**, 213 (2001).
18. D. Mishra, D.-J. Kim, J.-G. Ahn, and Y.-H. Rhee, Met. Mater. Int. **11**, 249 (2005).
19. G. Chauhan, K. K. Pant, and K. D. P. Nigam, Ind. Eng. Chem. Res. **52**, 16724 (2013).
20. D. Mishra, G. R. Chaudhury, D. J. Kim, and J. G. Ahn, Hydrometallurgy **101**, 35 (2010).
21. W. Mulak, A. Szymczycha, A. Lesniewicz, and W. Zyrnicki, Physicochem. Probl. Miner. Process. **40**, 69 (2006).
22. K. Mazurek, K. Białowicz, and M. Trypuć, Hydrometallurgy **103**, 19 (2010).
23. F. Beolchini, V. Fonti, F. Ferella, and F. Vegliò, J. Hazard. Mater. **178**, 529 (2010).
24. Y.-C. Lai, W.-J. Lee, K.-L. Huang, and C.-M. Wu, J. Hazard. Mater. **154**, 588 (2008).

25. I. M. Valverde Jr, J. F. Paulino, and J. C. Afonso, J. Hazard. Mater. **160**, 310 (2008).
26. K. H. Park, D. Mohapatra, and B. R. Reddy, J. Hazard. Mater. **138**, 311 (2006).
27. D. Santhiya and Y.-P. Ting, J. Biotechnol. **121**, 62 (2006).
28. K. H. Park, B. R. Reddy, D. Mohapatra, and C.-W. Nam, Int. J. Miner. Process. **80**, 261 (2006).
29. D. Santhiya and Y.-P. Ting, J. Biotechnol. **116**, 171 (2005).
30. S. P. Barik, K.-H. Park, P. K. Parhi, and J. T. Park, Hydrometallurgy **111**, 46 (2012).
31. H. Arslanoğlu and A. Yaraş, Pet. Sci. Technol. 1 (2019).
32. H.-I. Kim, K.-H. Park, and D. Mishra, Hydrometallurgy **98**, 192 (2009).
33. A. J. Chaudhary, J. D. Donaldson, S. C. Boddington, and S. M. Grimes, Hydrometallurgy **34**, 137 (1993).
34. A. Szymczycha-Madeja, J. Hazard. Mater. **186**, 2157 (2011).
35. T. E. Norgate, S. Jahanshahi, and W. J. Rankin, J. Clean. Prod. **15**, 838 (2007).
36. G. Chauhan, K. K. Pant, and K. D. P. Nigam, Environ. Sci. Process. Impacts **17**, 12 (2015).
37. J. Yang, Q. Zeng, L. Peng, M. Lei, H. Song, B. Tie, and J. Gu, J. Environ. Sci. **25**, 413 (2013).
38. S. Zhang, Z. Yang, B. Wu, Y. Wang, R. Wu, and Y. Liao, CLEAN–Soil, Air, Water **42**, 641 (2014).
39. A. C. Garrabrants and D. S. Kosson, Waste Manag. **20**, 155 (2000).
40. D. C. W. Tsang, W. Zhang, and I. M. C. Lo, Chemosphere **68**, 234 (2007).
41. W. Zhang, D. C. W. Tsang, and I. M. C. Lo, Chemosphere **66**, 2025 (2007).
42. W. Xia, H. Gao, X. Wang, C. Zhou, Y. Liu, T. Fan, and X. Wang, J. Hazard. Mater. **164**, 936 (2009).
43. W. Zhang, L. Tong, Y. Yuan, Z. Liu, H. Huang, F. Tan, and R. Qiu, J. Hazard. Mater. **178**, 578 (2010).
44. R. S. Tejowulan and W. H. Hendershot, Environ. Pollut. **103**, 135 (1998).
45. C. E. Martınez and H. L. Motto, Environ. Pollut. **107**, 153 (2000).
46. S. Goel, K. K. Pant, and K. D. P. Nigam, J. Hazard. Mater. **171**, 253 (2009).
47. K. R. Vuyyuru, K. K. Pant, V. V Krishnan, and K. D. P. Nigam, Ind. Eng. Chem. Res. **49**, 2014 (2010).
48. O. Alpaslan, A. Yaras, H. Arslanoglu, Bartın Univ. J. Eng. Technol. Sci. **7**, 18 (2019).
49. B. Nowack, Environ. Sci. Technol. **36**, 4009 (2002).
50. T. C. M. Yip, D. C. W. Tsang, and I. M. C. Lo, Chemosphere **81**, 415 (2010).
51. I. M. C. Lo, D. C. W. Tsang, T. C. M. Yip, F. Wang, and W. Zhang, Chemosphere **83**, 7 (2011).
52. W. Zhang and D. C. W. Tsang, Chemosphere **91**, 1281 (2013).
53. G. Chauhan, K. K. Pant, and K. D. P. Nigam, Ind. Eng. Chem. Res. **51**, 10354 (2012).
54. J. Singh and B.-K. Lee, Process Saf. Environ. Prot. **99**, 69 (2016).
55. S. Rao, T. Yang, D. Zhang, W. Liu, L. Chen, Z. Hao, Q. Xiao, and J. Wen, Hydrometallurgy **158**, 101 (2015).
56. C. Kim, Y. Lee, and S. K. Ong, Chemosphere **51**, 845 (2003).
57. A. Verma and S. Hait, Process Saf. Environ. Prot. **121**, 1 (2019).
58. P. Jadhao, G. Chauhan, K. K. Pant, and K. D. P. Nigam, Waste Manag. **57**, 102 (2016).
59. Z. Wang, S. Guo, and C. Ye, Procedia Environ. Sci. **31**, 917 (2016).
60. M. Authier-Martin, G. Forte, S. Ostap, and J. See, JOM **53**, 36 (2001).
61. M. Goto, B. C. Roy, and T. Hirose, J. Supercrit. Fluids **9**, 128 (1996).
62. Kn. C. Liddell, Hydrometallurgy **79**, 62 (2005).
63. C. Y. Wen, Ind. Eng. Chem. **60**, 34 (1968).
64. O. Levenspiel, Inc., New York (1972).
65. A. Ekmekyapar, E. Aktaş, A. Künkül, and N. Demirkiran, Metall. Mater. Trans. B Process Metall. Mater. Process. Sci. **43**, 764 (2012).